THE UNIVERSITY OF WARWICK

Permanent WRAP url:
http://wrap.warwick.ac.uk/62579

Publisher's statement:
Link to the published version: http://dx.doi.org/10.1038/ismej.2014.161

warwick**publications**wrap

highlight your research

http://wrap.warwick.ac.uk

Magnetic nanoparticle mediated isolation of functional bacteria in a complex microbial community

Running title: Recovering live uncultured bacteria *in-situ*

Dayi Zhang[a], James Berry[a], Di Zhu[a], Yun Wang[b], Yin Chen[c], Bo Jiang[d], Shi Huang[b], Harry Langford[a], Guanghe Li[d], Paul A. Davision[a], Jian Xu[b], Eric Aries[e] and Wei E. Huang[a]

[a] Kroto Research Institute, University of Sheffield, Sheffield, England, United Kingdom;

[b] Single-Cell Centre, CAS Key Laboratory of Biofuels and Shandong Key Laboratory of Energy Genetics, Qingdao Institute of BioEnergy and Bioprocess Technology, Chinese Academy of Sciences, Qingdao, China;

[c] School of Life Sciences, University of Warwick, Coventry, England, United Kingdom;

[d] School of Environment, Tsinghua University, Beijing, China;

[e] Tata Steel, Environment Technology, Group Environment, Swinden Technology Centre, Rotherham S60 3AR, United Kingdom.

*Corresponding author

Wei E. Huang

Tel: +44 (0)114 2225796 Fax: +44 (0)114 2225701

e-mail: w.huang@shef.ac.uk
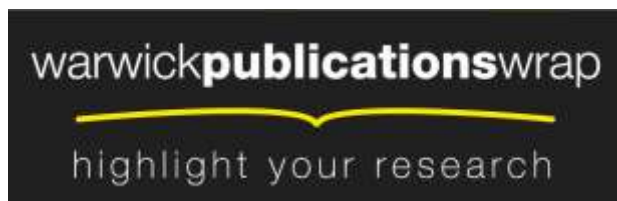
Abstract

Although uncultured microorganisms play important roles in ecosystems, their ecophysiology *in situ* remains elusive due to the difficulty of obtaining live cells from their natural habitats. In this study, we employed a novel magnetic nanoparticle mediated isolation (MMI) method to recover metabolically active cells of a group of previously uncultured phenol degraders, *Burkholderiales* spp., from coking plant wastewater biosludge; five other culturable phenol degraders – *Rhodococcus* sp., *Chryseobacterium* sp. and three different *Pseudomonas* spp. – were also isolated from the same biosludge using traditional methods. The kinetics of phenol degradation by MMI recovered cells (MRCs) was similar to that of the original sludge. Stable isotope probing (SIP) and pyrosequencing of the 16S rRNA from the ^{13}C-DNA fractions indicated that *Burkholderiales* spp. were key phenol degraders *in-situ* in the biosludge, consistent with the results of MRCs. Single cell Raman micro-spectroscopy was applied to probe individual bacteria in the MRCs from the SIP experiment and showed that 79% of them were fully ^{13}C-labelled. Biolog assays on the MRCs revealed the impact of various carbon and nitrogen substrates on the efficiency of phenol degradation in the wastewater treatment plant biosludge. Specifically, hydroxylamine (NH_2OH), a metabolite of ammonia oxidisation, but not nitrite, nitrate or ammonia, inhibited phenol degradation in the biosludge. Our results provided a novel insight into the occasional abrupt failure events that occur in the wastewater treatment plant. This study demonstrated that MMI is a powerful tool to recover live and functional cells *in-situ* from a complex microbial community to enable further characterisation of their physiology.

Key Words: magnetic nanoparticles | functionalisation | uncultured bacteria | Raman | single cell | stable isotope probing | biodegradation | hydroxylamine | phenol

Subject category: Microbial Ecology and functional diversity of natural habitats

Introduction

Around half of the total carbon in global biomass is present in microbes who play crucial roles not only in mediating global carbon and nitrogen cycles but also in regulating our climate (Schleifer 2004). However, the majority of microorganisms present in the environment remain uncultivated (Whitman et al 1998, Rappe and Giovannoni 2003), making it difficult to study their physiology. In addition, it is equally, if not more, important to study their functionalities and ecological roles in the biological context within their native microbial community.

It is a great challenge to understand the microbial physiology and *in situ* ecological roles of as yet uncultured bacteria. Several methods have been developed to study uncultured bacteria. Meta-approaches (*e.g.* metagenomics, metatranscriptomics, metaproteomics and metabolomics) (Handelsman 2004) circumvent the cultivation issue by extracting the total nucleic acids, proteins or chemicals from an environmental sample, and directly analysing them as a whole. These meta-approaches have given an unprecedented view of the diversity and complexity of microbial communities. Stable isotope probing (SIP) links uncultured microbial cells with the metabolism of specific stable isotope (^{13}C or ^{15}N) labelled substrates (Manefield et al 2002, Radajewski et al 2000). SIP combined with metagenomics is able to establish a connection between bacterial identity and ecological function (Chen and Murrell 2010, Wang et al 2012). SIP requires that stable isotopes such as ^{13}C and ^{15}N be incorporated into biomass (DNA, RNA or protein) and therefore has limited success in processes that have no incorporation of stable isotopes into biomass, such as nitrification, denitrification, sulphate reduction, iron reduction, methanogenesis, co-metabolism in consortia or mixed organic carbon anabolism (Bombach et al 2010, Nelson and Carlson 2012). Fluorescence *in-situ* hybridization and immunomagnetic cell capture have been used to isolate uncultured anaerobic methane oxidizing *Archaea* (Pernthaler et al 2008). More recently, single cell approaches have been developed to sort individual uncultured bacterial cells based on Raman or fluorescence signals, which can be subsequently coupled to single cell genomic analyses (Huang et al 2009, Read and Whiteley 2011, Rinke et al 2013, Wang et al 2013).

Although powerful, all these technologies are unable to recover live, functional cells of uncultured bacteria for further physiological study. A true understanding of

uncultured microorganisms requires the study of live cells in their natural environment. Given the complexity of the natural microbial community, it is difficult to target individual members of populations and separate them from the rest of the community. Various techniques have been developed to isolate and cultivate uncultured microorganisms, including dilution and modification of nutrient media, encapsulation of cells into beads or stimulation of cell growth (Kaeberlein et al 2002, Vartoukian et al 2010, Zengler et al 2002). Whilst these techniques have some success, one of the limitations of these techniques is the inability to study uncultured bacteria *in-situ*. It is thus desirable to identify and isolate functionally active, but as yet uncultured bacteria directly from their natural environment.

To address these challenges, in this study, a magnetic nanoparticle (MNP) mediated isolation (MMI) method was developed and employed to reveal active microbial cells that perform *in-situ* phenol degradation – *Burkholderiales* spp. – from coking plant wastewater. MMI recovered live cells (MRCs), which were dominant by *Burkholderiales* spp., were able to degrade phenol, showing a similar degradation kinetics to the original biosludge. The results of DNA stable isotope probing (SIP) and pyrosequencing of the ^{13}C-DNA fractions confirmed that *Burkholderiales* spp. were key degraders, whose sequences were >99% identical to the dominant species in MRCs. Single cell Raman micro-spectroscopy was used to examine individual cells in MRCs from the SIP experiment, which indicated that the majority (79%) of the individual cells in the MRCs were fully ^{13}C-labelled. All these results validated MMI method.

Biolog assays were applied to MRCs using various carbon and nitrogen substrates and revealed that a metabolite of the ammonia oxidisation pathway, hydroxylamine (NH_2OH), was as a key inhibitor that caused failure of phenol degradation in the coking wastewater treatment plant.

Materials and methods

Site description and sample collection

The coke oven biological wastewater treatment plant is operated by Tata Steel at Scunthorpe, UK. Main contaminants in the plant's influent are phenolic compounds, thiocyanate, polycyclic aromatic hydrocarbons (PAHs) and ammonia (50-70 mg/L), which are listed in Table S1. The average concentration of the major contaminant, phenol, was 250 mg/L. The operation temperature of the biological treatment unit was 25 $^{\circ}$C. Settled biosludge with normal and poor-performance from the activated sludge treatment tank were sampled and processed to set up microcosms on the same day. There was no detectable phenol in the supernatant of the settled sludge (Table S2). Biosludges of good and poor performance were designated as G-BS and P-BS respectively. The G-BS was sampled during periods of regular operation at the plant, whilst the P-BS was sampled just before a failure of water treatment that was associated with a sudden increase in nitrite concentration in the aeration tank (Fig. S1).

Isolation of phenol degraders from the biosludges by enrichment and cultivation

The raw biosludge was directly spread onto mineral medium (MM) agar plates with phenol (250 mg/L) as the sole carbon source. One litre of MM contained 2.5 g Na_2HPO_4, 2.5 g KH_2PO_4, 1.0 g NH_4Cl, 0.1 g $MgSO_4 \cdot 7H_2O$, 10 µL saturated $CaCl_2$ solution, 10 µL saturated $FeSO_4$ solution, and 1 mL Bauchop & Elsden solution (Bauchop and Elsden 1960). One percent (w/v) noble agar was used to prepare the MM agar (MMA) plates. The plates were incubated in the dark for 48 to 72 hours, and single colonies were identified and re-spread onto a MMA-phenol plate for further purification. The isolated strains were cultivated in MM-phenol liquid medium for nucleic acid extraction.

MNP synthesis and functionalisation of biosludges

MNP synthesis was carried out as previously described (Zhang et al 2011) with the following modifications. Briefly, 1 mL of $FeCl_2$ (1.0 M dissolved in 2.0 M HCl) and 2 mL of $FeCl_3$ (2.0 M dissolved in 2.0 M HCl) were mixed, to which 25 mL of NaOH (2.0 M) was slowly added drop by drop, with constant vortex mixing, for 30 minutes.

The synthesized MNPs were harvested by a permanent magnet and the supernatant was replaced with deionized water of the same volume. This washing step was repeated 6 times until the pH was neutral. Five mL of MNPs were then mixed with 45 mL of polyallylamine hydrochloride (PAAH) solution (10 mg/mL), which was then stabilized for 60 minutes in an ultrasound bath with 40-kHz and an output energy of 75 W (Langford Electronics Ltd., Coventry, UK). After centrifugation at 10,000 g for 10 minutes, the pellet was re-suspended in 50 mL deionized water and well-dispersed by vortex mixing. The final solution was passed through a 0.2 μm filter (Millipore, USA) and was then ready for bacterial functionalisation. PAAH is a cationic polyelectrolyte, contributing positive charge to the MNPs and maintaining their dispersion in the water.

A schematic for cultivating bacteria from biosludge through MMI is shown in Fig. 1. First, all cells from the biosludge were functionalised by mixing biosludge with biocompatible MNPs. Ten mL of biosludge (G-BS and P-BS) was centrifuged at 3,000 rpm for 10 minutes and the bacterial pellet was harvested and resuspended in the same volume of deionized water. The cell suspension was mixed with 10 mL of PAAH-stabilized MNP solution. The bacteria-MNP mixture was incubated at room temperature for 20 minutes with shaking (150 rpm). The MNP functionalised bacteria were then separated from the aqueous phase by a permanent magnet, followed by resuspension in deionized water. The washing step was repeated three times to remove those bacteria that were not functionalised by MNPs. Subsequently, the MNP functionalised bacteria were resuspended in 10-ml filter-sterilised wastewater. To prepare filtered-sterilised wastewater, G-BS was centrifuged at 4,000 rpm for 10 minutes and the supernatant was passed through 0.2 μm filters twice to remove cells.

The MNP-cells were then re-introduced into filter-sterilised wastewater in which 250 mg/L phenol ($^{13}C_6$ and ^{12}C- phenol) was added as the carbon source. In the presence of phenol, active phenol degraders divided, causing the MNPs coated onto the cells were gradually diluted and its magnetic attraction eventually lost. After phenol degradation was completed, a permanent magnet was re-applied. The active phenol degraders were freely suspended in the water phase, whilst the rest of cells (non-divisive or inactive phenol degraders) were attracted and immobilised by the magnet (Fig. 1). In this way live bacterial cells responsible for phenol degradation *in-situ* can be recovered by this MMI method.

178   *Phenol degradation in microcosms*

179   For *in-situ* phenol degradation experiments a series of treatments were carried out,

180   including: phenol blank control (no biosludge), original biosludge control (no phenol),

181   original biosludge supplemented with water (negative control), ^{13}C- or ^{12}C- phenol

182   (final concentration 250 mg/L), filter-sterilised biosludge mixed with MNP-cells

183   supplemented with water (negative control), ^{13}C- or ^{12}C- phenol (final concentration

184   250 mg/L). Three replicates were carried out for each treatment. Samples were taken

185   every 30 minutes from the incubations using G-BS and every hour from those using

186   P-BS to determine the residual phenol concentrations. A subset of samples (0.5 mL)

187   were taken from ^{13}C and ^{12}C-phenol amended G-BS microcosms at t= 0, 2.5, 5 and 7

188   hours, which were used for latter DNA-SIP analyses of active microbial populations

189   involved in phenol degradation. Phenol concentration was measured by a

190   spectrophotometric method described by the American Public Health Association

191   (Greenberg et al 2005). Briefly, 100 µL of cell-free sample was diluted in 900 µL

192   deionized water, dosed in the following order with 400 µL of 2.0 M NH_4OH, 200 µL

193   of 2% (w/w) aminoantipyrine and 400 µL of 2% (w/w) $K_3Fe(CN)_6$. The absorbance of

194   the mixture was then measured at 500 nm wavelength using a microplate reader

195   (Synergy II multimode, BioTek Instruments, Inc., USA).

196

197   *MNP mediated cell isolation and counting*

198   After completion of phenol degradation, MRCs in the suspension were stained by

199   4',6-diamidino-5-phenyl-indole (DAPI) (Kubista et al 1987) and counted under a

200   Zeiss Axioplan 2 epifluorescence microscope. MRCs in the suspension were

201   centrifuged at 3,000 rpm for 10 minutes and resuspended in the same volume of

202   phosphate-buffered saline (PBS, 54.44 mg KH_2PO_4 and 106.8 mg $Na_2HPO_4 \cdot 12H_2O$ in

203   10 mL deionized water). To enumerate the population of MRCs, 20 µL of the cell

204   suspension was diluted to 1 mL with autoclaved UHQ water, buffered with PBS. This

205   dilution was then incubated in the dark with DAPI stain, corresponding to a working

206   concentration of 12.5 µg/mL, filtered onto a 0.2 mm black polycarbonate filter paper

207   and mounted onto a glass slide with Fluoroshield™ mounting medium (Sigma). The

208   resultant slides were analysed and imaged under fluorescent light using the

209 microscope with a DAPI filter cube. The cells were detected using 358-nm UV light

210 for excitation and 461 nm for emission. In order to determine the cell density of the

211 supernatant, cell counts were performed for 15 randomly chosen fields of view. For

212 means of comparison, a 10^{-4} dilution of the original biosludge was enumerated using

213 the same approach.

214

215 *Physiological testing of MRCs using the Biolog high-throughput phenotypic assay*

216 Biolog plate (BIOLOG, USA) analyse were undertaken to examine the carbon and

217 nitrogen metabolism of MRCs. *Pseudomonas putida* XY5 isolated from the same

218 biosludge was used as a control. Biolog PM1 plate was used for carbon metabolism

219 and PM3 for nitrogen metabolism in accordance with the manufacturer's instructions.

220 The coking wastewater naturally contains a high concentration of ammonia and

221 operator experience found that a failure of treatment was always associated with the

222 presence of nitrite in the aeration tank, which suggests that the nitrogen source could

223 affect phenol biodegradation. Hence, for the PM3 nitrogen assay, 250 mg/L phenol

224 was used as the carbon source to reveal the effect of nitrogen sources on phenol

225 degradation.

226

227 *The effect of nitrogen source on phenol biodegradation*

228 Ammonium chloride, sodium nitrite, sodium nitrate and hydroxylamine were added

229 into filter-sterilised wastewater (from G-BS) as nitrogen sources. The background

230 concentrations of phenol and nitrogen sources are shown in Table S2. All samples

231 were set up in triplicate. Phenol was added into all treatments with a final

232 concentration of 250 mg/L. The final concentrations of NH_3-N, NO_2^- and NO_3^- were

233 232 mg/L (100 mg/L amendment with background 132 mg/L shown in Table S2), 50

234 mg/L, and 100.23 mg/L (100 mg/L amendment with background 0.23 mg/L shown in

235 Table S2), respectively. The final concentrations of NH_2OH were 0.1, 0.2, 0.5, 1.0,

236 2.0, 5.0 and 10 mg/L. Samples were added into a 96-well microplate: each well

237 contained 160 µL of filter-sterilised wastewater, 20 µL of appropriate phenol with

238 nitrogen compounds (or water), and 20 µL of cell suspension of MRCS (or water).

239 The microplate was incubated at 25 ^{o}C in the microplate reader and OD_{600} was

240 recorded every 15 minutes. At the end of incubation, the pH values in each sample

241 were measured using indicator strips. Residue phenol concentration was measured
242 according to the method described above, and the percentage of phenol degradation
243 was calculated by final concentration relative to the three cell-free controls on the
244 same plate.

245

246 *Detection of single cells in MRCs by Raman micro-spectroscopy*

247 Raman micro-spectroscopy was employed to quantify ^{13}C-incorporation of MRCs at
248 the single cell level (Huang et al 2004, Huang et al 2007, Huang et al 2009). MRCs
249 were harvested from the above treatments. MRCs were centrifuged at 3,500 rpm for
250 10 minutes, and washed with water three times. Each cell suspension (2~5 µL) was
251 spread onto a calcium fluoride (CaF$_2$) slide and allowed to air dry prior to Raman
252 analysis. Single cell Raman spectra (SCRS) were acquired using a confocal Raman
253 microscope (LabRAM HR, HORIBA Scientific, UK). A 100× magnifying dry
254 objective (NA=0.90, Olympus, UK) was used to observe and acquire Raman signals
255 from single cells. The Raman scattering was excited with a 532-nm Nd:YAG laser
256 (Torus Laser, Laser Quantum, UK). The laser power on a single cell was about 15
257 mW. Each Raman spectrum was acquired between the range of 1989 cm^{-1} to 336 cm^{-1},
258 with 1021 data points and a resolution of ~1 cm^{-1}. LabSpec software (HORIBA
259 Scientific, UK) was used to operate the Raman system and acquire Raman spectra.
260 Acquisition time was 20 s for measurement of each single cell.

261

262 *Nucleic acid extraction*

263 The biosludge samples were collected at the beginning and the end of phenol
264 degradation. Total nucleic acids were extracted from 1.0 mL of each biosludge sample
265 or culture of the isolated phenol degraders using a PowerSoil DNA Isolation Kit (MO
266 BIO, USA) according to the manufacturer's instructions.

267

268 *DNA-stable Isotope Probing (DNA-SIP)*

269 ^{13}C-labelled 'heavy' DNA was separated from unlabelled ^{12}C DNA ('light' DNA) by
270 equilibrium density gradient centrifugation using a protocol described by Neufeld et
271 al. (2007). Briefly, 1 µg of DNA was mixed with the CsCl gradient buffer to a volume

272 of 1.2 mL, to which 4.6 mL of 7.163 M CsCl solution was added to obtain a final

273 density of 1.725 g/mL. The mixture was inverted gently and transferred into a 5.8-mL

274 ultracentrifuge tube (Beckman). After balancing and sealing, the tubes were spun in

275 an ultracentrifuge (Optima L-80 XP, Beckman Coulter) at 44,100 rpm (~177,000 g,

276 VTi65.2 rotor, Beckman) for 40 hours. The DNA of different density was retrieved by

277 gradient collection into 12 fractions of 400 µL volume from the bottom of the

278 ultracentrifuge tube. The injection of deionized water was manipulated to push down

279 fractions from the top of the ultracentrifuge tube by a low-flow peristaltic pump

280 (Watson Marlow Ltd.). The DNA fractions were then purified by glycogen and PEG

281 6000 solution for 2 hours, washed with 70% ethanol, air-dried and dissolved in 50 µL

282 DNase-free water. The DNA from the ^{12}C phenol control was manipulated with the

283 same centrifugation, fractionation and purification procedures.

284

285 *PCR amplification of 16S rRNA genes and phenol hydroxylase genes*

286 PCR amplification was carried out in a C1000 thermal cycler (Thermo, USA). Each

287 reaction (50 µL) contained 0.5 µL Dream Taq DNA polymerase (Promega, USA), 5

288 µL deoxynucleotide triphosphates at a concentration of 10 mM, 2.5 µL of each primer,

289 1 µL DNA template and 38.5 µL molecular water. For MRCs, 1 µL cell suspension

290 was directly used as the DNA template for the amplification of 16S rRNA genes.

291 DNA fragments of 16S rRNA genes were amplified by the primer pair of 63f and

292 1387r, as listed in Table 1. After 94°C for 10 minutes, 35 cycles were undertaken with

293 94°C for 1 minute, 56°C for 1 minute, and 72°C for 1 minute, followed by a final

294 extension at 72°C for 10 minutes. The largest subunit of the multicomponent phenol

295 hydroxylases (LmPH) was amplified using different primer sets targeting three

296 different types of phenol hydroxylases (Futamata et al., 2001). For the primer pair of

297 phe1f/phe3r (Table 1), the PCR program used was as follows: 10 minutes at 94°C; 35

298 cycles of 94°C for 1 minute, 56°C for 1 minute, and 72°C for 1.5 minutes; final

299 extension at 72°C for 10 minutes. The PCR program for the primer pheUf/pheMHr

300 and pheUf/pheHr was as follows: 94°C for 10 minutes; 5 cycles of 94°C for 1 minute,

301 58°C for 1 minute, and 72°C for 1 minute; 5 cycles of 94°C for 1 minute, 57°C for 1

302 minute, and 72°C for 1 minute; 25 cycles of 94°C for 1 minute, 56°C for 1 minute,

303 and 72°C for 1 minute; 72°C for 10 minutes as final extension. For the primer set

304 pheUf/pheLr, the program was: 94°C for 10 minutes; 5 cycles of 94°C for 1 minute,

305 55°C for 1 minute, and 72°C for 1 minute; 5 cycles of 94°C for 1 minute, 54°C for 1

306 minute, and 72°C for 1 minute; 25 cycles of 94°C for 1 minute, 53°C for 1 minute,

307 and 72°C for 1 minute; 72°C for 10 minutes as final extension. The PCR products

308 were checked by electrophoresis on a 1.5% (w/v) agarose gel (Sigma) using TBE

309 buffer.

310 To determine the diversity of microbes in MRCs, the 16S rRNA PCR products from

311 MRCs were cloned into pGEM-T vector (Promega, USA), and transferred into *E. coli*

312 JM109 competent cells by heat shock. Thirty clones were randomly selected for

313 plasmid extraction and the 16S rRNA inserts were sequenced.

314

315 *Nucleotide sequencing and computational analysis*

316 PCR amplicon libraries of the hypervariable V1-V3 region of the 16S rRNA genes

317 (corresponding to *Escherichia coli* positions 5-534) were generated for 'heavy' and

318 'light' DNA fractions of the DNA-SIP incubations (t=0, 2.5, 5 and 7 hr, respectively).

319 PCR was performed using the forward primer (NNNNNNN-

320 TGGAGAGTTTGATCCTGGCTCAG) and reverse primer (NNNNNNN-

321 TACCGCGGCTGCTGGCAC). Unique heptad-nucleotide sequences (seven bases)

322 were synthesized at the 5' end of each pair of primers as barcodes, which were used to

323 assign sequences to different samples. Pyrosequencing was carried out using a

324 Genome Sequencer FLX Titanium platform (Roche, USA) where reads of on average

325 400 bp in length were produced.

326 In quality filtering, reads were discarded if they were shorter than 150 bp, or longer

327 than 1,000 bp, had an average quality score of < 35 in each 50-bp window rolling

328 along the whole read, or contained primer mismatches, uncorrectable barcodes,

329 ambiguous bases or homopolymer runs in excess of 8 bases. Sequences that passed

330 the quality filters were then analysed using the MOTHUR software package (Schloss

331 et al 2009). Sequences were assigned to operational taxonomic units (OTUs) with a

332 97% pairwise identity as the threshold, and then classified taxonomically using the

333 Greengenes16S rRNA reference database (McDonald et al 2012) with a confidence

334 threshold of $> 80\%$. The Greengenes taxonomies were used to generate summaries of

335 the taxonomic distributions at different phylogenetic levels. To standardize sequence

336 counts across samples with uneven sampling, we randomly selected 2008 sequences

per sample (rarefaction) and used this as a basis to compare abundances of OTUs across samples. The Bray-Curtis metric was used to generate distance matrices from samples, which were visualized as a PCoA (Principal Coordinates Analysis) plot and a dendrogram based on the UPGMA algorithm.

To assess the abundance of ^{13}C-DNA fraction in the samples, pyrosequencing reads were aligned to the reference sequence (an uncultivated *Burkholderiales* spp. Genbank accession no. KM067154), the representative sequence of the dominant OTU in MRCs) with BLASTN. Distribution of the sequence similarity of these alignments were visualized as histograms, in which were compared the match of the *Burkholderiales* spp. reference sequence to $^{12C\text{-}DNA}$ and ^{13}C-DNA fractions at the two time points at 0 and 7 hours of phenol degradation.

The 454 reads that were taxonomically assigned to the order Burkholderiales using Greengenes database were clustered into operational taxonomic units (OTUs) with a 97% pairwise identity as the threshold. The representative sequences of all 12 OTUs in the ^{13}C-DNA fraction were then aligned to the *Burkholderiales* spp. reference sequence (Genbank accession no. KM067154), which was identified in MRCs using MUSCLE. For phylogenetic analysis, a maximum likelihood (ML) tree was built with 1000 bootstrappings in MEGA6.

DNA sequences of 16S-rRNA gene and phenol hydroxylase from this study are available in Genbank (accession number KM067152 to KM067154 and KJ174591 to KJ174607).

Results

Isolation of culturable phenol-degrading microorganisms

361 *Rhodococcus* sp. XY2, *Chryseobacterium* sp. XY3 and three different *Pseudomonas*

362 strains (XY4, XY5 and XY6) were isolated on agar plates from the biosludge samples

363 (Table S3) using minimal medium with phenol as the sole carbon source. The 16S

364 rRNA sequences of *Pseudomonas* sp. XY4 and XY5 are identical (100%) to that of

365 *Pseudomonas pseudoalcaligenes* and *Pseudomonas putida* KT2440 respectively,

366 while the 16S rRNA of *Pseudomonas* sp. XY6 is 99.6% identical to that of

367 *Pseudomonas plecoglossicida*. However, subsequent culture-independent analyses

368 suggest that these isolates were not responsible for phenol biodegradation *in-situ*.

369

370 *MNP-functionalisation of biosludges do not affect the rates of phenol degradation*

371 The rates of phenol degradation of two biosludge samples of contrasting

372 performances (G-BS and P-BS) were determined in order to assess the impact of

373 MNP on phenol degradation. The data are shown in Figure 2A. After 7 hours, the

374 microbial community in G-BS degraded phenol completely (Fig. 2A). In contrast, no

375 phenol degradation occurred in P-BS in the initial 18 hours and phenol degradation

376 was not completed until 36 hours (Fig. 2A). The use of stable-isotope labelled phenol

377 (^{13}C-phenol) had no impact on the performance of phenol degradation using the two

378 biosludges samples (Fig. 2A). MNP-functionalised biosludges had similar rates of

379 phenol degradation compared to those of the raw biosludges, confirming that MNP

380 functionalisation is biocompatible (Fig. 2A).

381

382 *MRCs had a similar performance as the whole biosludge for phenol degradation*

383 The MNP-functionalised cells were introduced into filter-sterilised wastewater to

384 allow for propagation of active phenol degraders in their natural environment. Either

385 ^{13}C-labelled phenol or ^{12}C-phenol or water as positive and negative controls were

386 added to the MNP-functionalised cells. In these experiments, there were no free cells

387 in treatments at time point T=0. After phenol degradation was completed (Fig. 2A),

388 MRCs were magnetically separated from the treatments. DAPI staining of MRCs

389 from the ^{13}C- or ^{12}C- phenol treatment showed that the cell population was 1.48 $\pm$

390   0.49×10^5 cells/mL. In contrast, the cell density in controls where phenol was not

391   added was two orders of magnitude lower ($<10^3$ cells/mL) which excludes the

392   possibility that MNPs were lost due to some random reason. In comparison, the total

393   cell population in the original biosludge was $1.05 \pm 0.64 \times 10^9$ cells/mL. The DAPI

394   counting approach may underestimate the cell population because the cell-harvesting

395   step using centrifugation at 3,000 rpm for 10 min may miss small cells that are not

396   easily pelleted.

397   The MRCs derived from MNP treated biosludges were incubated with phenol (250

398   mg/L) to determine if they were functionally active. The data presented in Fig. 2B

399   demonstrate that the degradation pattern was similar to that of the original raw

400   biosludges (G-BS) after a 2 hours delay (Fig. 2B). MRCs from the controls (no phenol

401   amendment) had no phenol degradation activity (data not shown). This suggested that

402   the active phenol degraders responsible for phenol degradation in the original raw G-

403   BS should be recovered in MRCs.

404

405   *Raman micro-spectroscopy analyses of MRCs confirmed ^{13}C incorporation at the*

406   *single cell level*

407   MRCs from ^{13}C and ^{12}C-phenol treatments were examined by Raman micro-

408   spectroscopy at the single cell level. SCRS of MRCs were acquired to examine their

409   ^{13}C-incorporation, based upon the fact that some Raman bands of ^{13}C-labelled cells

410   shift to lower wavenumbers upon the incorporation of ^{13}C from a growth substrate

411   (Huang et al 2004, Huang et al 2007, Huang et al 2009, Li et al 2013). SCRS of

412   MRCs from ^{12}C-phenol treatments were used as 12C- unlabelled controls.

413   Microscopic images indicated that cells from MRCs were more uniform than those in

414   the original biosludge. MRCs were mostly rod-shaped and of similar sizes and Raman

415   spectral patterns (Fig. 3). SCRS from the cells with ^{13}C incorporation showed

416   significant Raman shifts in the marker bands namely the phenylalanine band, from

417   1001.8 to 965.7 cm^{-1} and the protein band, from 1668.6 cm^{-1} to 1626.1 cm^{-1}

418   respectively (Fig. 3). Other Raman bands such as 641, 723, 781, 1121, 1317, and

419   1576 cm^{-1} also shifted in a similar way due to the incorporation of ^{13}C into the cells

420   (Fig. 3). Analysis of Raman spectra of 135 randomly selected single cells in the

421   MRCs from the ^{13}C-phenol treatment indicated that 79% of MRCs were fully labelled

with ^{13}C (Fig. 3). These results indicated that most freely-suspended cells from the MRCs were indeed active phenol degraders.

Uncultured Burkholderiales *spp. were responsible for phenol degradation*

DNA sequencing of 30 clones of 16S rRNA PCR products using MRCs as the DNA template suggested that 67% of bacteria in MRCs were related to an uncultivated *Burkholderiales* spp. (12 identical clones accession number: KM067154 and 8 identical clones accession number: KM067153). Interestingly, this is a new group of bacteria showing <92% identity to all prokaryotic 16S ribosomal RNAs in the NCBI database.

Pyrosequencing of DNA-SIP samples indicated that the dominant bacteria in the $^{13C\text{-}DNA}$ fractions were unclassified *Burkholderiales* spp. (Fig. 4A). Microbial community structure changed over time and by the time of complete phenol degradation at 7 hours, the microbial structure had changed significantly in that the $^{13C\text{-}DNA}$ fraction was different from the rest of the microbial community structures (Fig. 4B).

The representative sequences of 12 *Burkholderiales* spp. OTUs were identified and the dominant sequence was OTU34. (Fig. S3A). A comparison between the sequence of KM067154 and OTU34 showed that they are 99% identical. A phylogenetic tree was generated using the sequences of the 12 OTUs representing *Burkolderiales* spp. and the dominant *Burkholderiales* spp. (accession number: KM067154) independently found in the MRCs (Fig. S3B). It showed that SIP and MRC derived data are highly consistent, indicating that the uncultivated *Burkholderiales* spp. was active and responsible for phenol degradation *in situ* (Fig. S3B). The advantage of MRCs is that live cells were obtained which can be used for further physiological study.

The 16S-rRNA sequences of *Burkholderiales* spp. (accession number: KM067154) were also used as a reference and aligned to all pyrosequences of ^{12}C-DNA and ^{13}C-DNA fractions at time 0 and 7 hours degradation time. The histogram clearly showed that more than 60% readings of ^{13}C-DNA fraction at 7 hours were identical (>99% identity) to *Burkholderiales* spp. sequences obtained from MRCs (Fig. S2).

Diversity of functional genes for phenol degradation

454 A key functional gene for phenol degradation is phenol hydroxylase, which converts
455 phenol into catechol before prior to the TCA cycle. Phenol hydroxylase can be
456 recovered by PCR using degenerate primers (Table 1). Table S3 summarises the
457 occurrence of phenol hydroxylase genes in different samples.

458 In the original biosludges (both the BS-G and BS-P samples), all four types of LmPH,
459 *phe1, pheMH*, *pheL* and *pheH*, were found. The phenol hydroxylase genes in the
460 MRCs and ^{13}C fraction belong to the *Burkholderiales* order; More specifically, the
461 *phe1* and *pheL* (accession number KJ174604 and KJ174605) genes in the MRCs are
462 identical to those of *Cupriavidus metallidurans* CH34 (formerly *Ralstonia*
463 *metallidurans* Janssen et al 2010) (Table S3).

464 In the cultivated species isolated from the biosludges however, the phenol
465 hydroxylase genes were of different types. Specifically, *Chryseobacterium* sp. XY3
466 has an identical *pheL* (a phenol hydroxylase subunit gene) to that of *Comamonas* sp.
467 J5-66 (Sun et al 2012). The isolated *P. pseudoalcaligenes* XY4 and *P. plecoglossicida*
468 XY6 have two domains of LmPH (*phe1* and *pheMH*) (accession number KJ174598
469 and KJ174600), which were both identical to that in *Pseudomonas* sp. (Table S3)
470 (Kim et al 2005). Interestingly, it was found that *P. putida* XY5 contained novel types
471 of phenol hydroxylase, *phe1* and *pheMH* (accession number KJ174599) that have not
472 been reported previously.

473

474 *Phenotyping MRCs*

475 A remarkable advantage of MMI is that it enables the isolation of live bacteria for
476 ecophysiological analysis. Biolog high-throughput phenotypic microarrays were used
477 for the phenotypic analysis of MRCs. They served two purposes: the characterisation
478 of phenotypes and the identification of key factors affecting the performance of
479 phenol degradation. The MRCs and *P. putida* XY5 showed different phenotypic
480 patterns for carbon metabolism (Table S4), providing additional evidence that the
481 bacteria isolated using the MMI technique were different from those readily cultivated
482 phenol degraders such as *P. putida.* Specifically for MRCs, the carbon sources, such
483 as D-alanine, α-D-glucose, tyramine and L-glutamine, promoted cell growth, whereas

484   the carbon sources, such as D-galactonic acid-γ-lactone, L-galactonic acid-γ-lactone,

485   m-tartaric acid and D-threonine, inhibited cell growth (Table S4).

486   To examine the impact of nitrogen sources on biodegradation performance, phenol

487   (250 mg/L) was used as the carbon source in the PM3 nitrogen test plates. Data

488   presented in Table S5 showed that MRCs and *P. putida* XY5 had different response

489   patterns to different nitrogen sources. NH_2OH and D,L-α-amino-caprylic acid

490   significantly inhibited phenol degradation in both MRCs and *P. putida* XY5, whilst

491   ammonia, nitrite and nitrate did not show any repression effect on phenol degradation

492   (Table S5).

493

494   *Hydroxylamine is an inhibitor for phenol degradation in coke oven biosludges*

495   The ammonia concentration in the influent wastewater was 50-70 mg/L (Table S1)

496   and 132 mg/L in the settled sludge (Table S2) generated from thiocyanate (SCN^-)

497   degradation. It was observed that the failure of wastewater treatment was associated

498   with a sudden increase of nitrite (Fig. S1). Ammonia and its metabolic intermediates

499   compounds NH_2OH, NO_2^- and NO_3^- were added into the filter-sterilised wastewater

500   along with MRCs within which *Burkholderiales* spp. were enriched. During 19 hours

501   of incubation, the pH in the media of all treatments remained between 6.4-6.8,

502   indicating that metabolism of NH_2OH, nitrite, nitrate and ammonia did not alter the

503   pH of the media. Cell growth in the treatment with NH_2OH >5 mg/L was inhibited

504   whilst cells with 232 mg/L NH_3-N, 50 mg/L NO_2^-, 100.23 mg/L NO_3^- and <2 mg/L

505   NH_2OH continued to grow (Fig. 5A). Phenol concentration remained unchanged after

506   19 hours incubation when NH_2OH was greater than 5 mg/L, whilst phenol was

507   completely degraded in the other treatments (Fig. 5B). The results indicated that a

508   NH_2OH concentration greater than 5 mg/L completely inhibited phenol degradation

509   by *Burkholderiales* spp., whilst 50 mg/L NO_2^-, 100.23 mg/L NO_3^- and 232 mg/L NH_3-

510   N did not inhibit phenol degradation (Fig. 5).

511

Discussion

It is increasingly evident that as yet uncultured bacteria can play key roles in the biodegradation and bioremediation of environmental pollutants (Huang et al 2009, Read and Whiteley 2011, Chen and Murrell 2010, Wang et al 2012). In this study, we demonstrated that MMI can be used to recover live cells of key pollutant degraders from a complex microbial community such as biosludge and that MRCs can be used for further eco-physiological studies. MRCs were able to degrade phenol and had a similar degradation pattern to the original biosludge. Fully ^{13}C- labelled phenol of ambient concentration was introduced into the biosludge to probe the *in-situ* active degraders. Subsequent recovery of MRCs and Raman micro-spectroscopy analyses at the single cell level demonstrated that the majority of MRCs were indeed labelled by ^{13}C, indicating that they play a key role in phenol degradation. These data are consistent to the results from the DNA-SIP analyses: sequencing and phylogenetic analyses indicated that the major species in the ^{13}C-DNA fraction of the biosludge was related to a group of so-far uncultivated *Burkholderiales* spp., which showed high sequence identity (>99%) to the predominant 16S rRNA gene retrieved from clone library analysis of MRCs. Collectively, our results demonstrated that the MMI method was powerful in identifying and isolating a new group of *Burkholderiales* spp. as the key phenol degraders in these biosludges.

This methodology builds on the fact that cell division of the active bacterial cells will dilute MNP coatings and ultimately result in a loss of magnetic attraction. Conversely, the metabolically inactive bacteria keep their MNPs and thus remain magnetically attractive. To enable effective isolation of these two groups of cells in a complex community, the following properties for MNPs are essential (Zhang et al 2011) – they need to be: 1) biocompatible – MNPs should have minimal impact on cell physiology in terms of growth and enzymatic activities; 2) magnetically controllable – MNP-functionalised cells can be easily manipulated by a magnetic field, which requires a suitable MNP size and MNP-to-cell ratio; 3) highly efficient for functionalisation – MNP coating efficiency is greater than 99.9%, ensuring that almost all cells in a microbial community can be magnetically functionalised; 4) dilutable – MNPs coated on cells can be diluted and eventually lost after cell divisions. Whilst the MMI approach has been shown to be powerful in this study, it has its own limitations. So far, the MMI approach is only effective in the recovery of actively dividing and

545 rapidly growing bacteria that are capable of escaping the MNPs within a given time. It
546 remains to be established whether MMI can be used to separate active, but slow
547 growing bacteria or those who can turn over the substrate without cell division.

548 The operation data of the coking plant's wastewater treatment suggested that a sudden
549 increase of NO_2^- in the wastewater was often associated with a sudden drop in the
550 removal efficiency of chemical oxygen demand and subsequent failure of water
551 treatment (Fig. S1). It was observed that the treatment often failed when NO_2^-
552 concentration was greater than a threshold of 10 mg/L. For example, at the point of
553 high NO_2^- concentration (>10 mg/L) in Nov 2012, a failure of water treatment
554 occurred along with the appearance of P-BS (Fig. S1). The P-BS was still able to
555 degrade phenol but there was a long lag time (18 hours) before phenol degradation
556 occurred (Fig. 2A). This implied that nitrogen metabolism by the biosludge microbial
557 community affected wastewater treatment performance. Hence, in the Biolog PM3
558 nitrogen metabolism test, phenol (250 mg/L) was used as the sole carbon source to
559 examine the impact of nitrogen metabolism on the phenol degrading ability of
560 uncultured but metabolically active microbial cells. Figure 6A indicated that $NH_2OH >$
561 5mg/L completely inhibited phenol degradation, whilst 50 mg/L NO_2^- did not inhibit
562 phenol degradation. Both ammonia-oxidizing *Archaea* and ammonia-oxidizing
563 *Bacteria* oxidise NH_3 into NH_2OH (Arp et al 2002, Vajrala et al 2013), which is then
564 further oxidised to nitrite (NO_2^-) and finally nitrate (NO_3^-). The experimental data
565 clearly indicated that it was NH_2OH, but not NO_2^-, NO_3^- or NH_3, that inhibited phenol
566 degradation in the coking wastewater. The threshold of this NH_2OH inhibition effect
567 was between 2 and 5 mg/L (Fig. 5). It is likely, therefore, that the high concentration
568 of NO_2^- within the wastewater treatment facility was a result of NH_2OH accumulation
569 and it was NH_2OH that led to the failure in wastewater treatment. NH_2OH is a volatile
570 and unstable compound and in fact, when its concentration decreased below the
571 threshold, phenol biodegradation resumed (Fig. 2A). Presumably, the degradation of
572 thiocyanate (120-250 mg/L in the influent, Table S1) would produce ammonia via
573 $SCN^- \rightarrow SO_4^{2-}+NH_3+CO_2$, which could lead to an increase in ammonia during the
574 wastewater treatment (e.g. 132 mg/L in settled sludge shown in Table S2) compared
575 with 50-70 mg/L ammonia in the influent (Table S1). The accumulation of NH_2OH is
576 likely due to the low activity of hydroxylamine oxidoreductase which catalyses the
577 formation of NO_2^-.

578 To summarize, we demonstrate that live and uncultured bacteria can be recovered
579 using this novel MMI approach. It is foreseeable that this MMI approach will greatly
580 accelerate the pace of exploration for as yet uncultured microbes, and help our
581 understanding of the diversity, physiology, functional potential, evolution, adaptation
582 and ecophysiology of the microbes present in the environment. MMI enriched
583 uncultured cells can be subjected to single cell isolation and genome assembly.

584

593

594 **Conflict of Interest**

595 The authors declare no conflict of interest.

596

597 **Author contributions**

598 WEH, DZ and EA designed the research. DZ, WEH, JB, DZ (Di Zhu), HL, BJ, GL
599 and YC performed the experiments. DZ and WEH analysed data. YW, SH and JX
600 undertook computational analysis. WEH, DZ and YC wrote the paper.

601

602 **Supplementary information**

603 Supplementary information is available at ISMEJ's website at the end of the article
604 and before the references.

Reference

Arp DJ, Sayavedra-Soto LA, Hommes NG (2002). Molecular biology and biochemistry of ammonia oxidation by *Nitrosomonas europaea*. *Arch Microbiol* **178:** 250-255.

Bauchop T, Elsden SR (1960). The growth of micro-organisms in relation to their energy supply. *J Gen Microbiol* **23:** 457-469.

Bombach P, Chatzinotas A, Neu TR, Kaestner M, Lueders T, Vogt C (2010). Enrichment and characterization of a sulfate-reducing toluene-degrading microbial consortium by combining in situ microcosms and stable isotope probing techniques. *FEMS Microbiol Ecol* **71:** 237-246.

Chen Y, Murrell JC (2010). When metagenomics meets stable-isotope probing: progress and perspectives. *Trends Microbiol* **18:** 157-163.

Futamata H, Harayama S, Watanabe K (2001). Group-specific monitoring of phenol hydroxylase genes for a functional assessment of phenol-stimulated trichloroethylene bioremediation. *Appl Environ Microbiol* **67:** 4671-4677.

Greenberg AE, Clesceri LS, Eaton AD (2005). *Standard methods for the examination of water and wastewater*. Washington, DC: American Public Health Association (APHA).

Handelsman J (2004). Metagenomics: Application of genomics to uncultured microorganisms. *Microbiol Mol Biol Rev* **68:** 669-685.

Huang WE, Griffiths RI, Thompson IP, Bailey MJ, Whiteley AS (2004). Raman microscopic analysis of single microbial cells. *Anal Chem* **76:** 4452-4458.

Huang WE, Stoecker K, Griffiths R, Newbold L, Daims H, Whiteley AS *et al* (2007). Raman-FISH: Combining stable-isotope Raman spectroscopy and fluorescence in situ hybridization for the single cell analysis of identity and function. *Environ Microbiol* **9:** 1878-1889.

Huang WE, Ferguson A, Singer AC, Lawson K, Thompson IP, Kalin RM *et al* (2009). Resolving genetic functions within microbial populations: In situ analyses using rRNA and mRNA stable isotope probing coupled with single-cell Raman-fluorescence *in situ* yybridization. *Appl Environ Microbiol* **75:** 234-241.

Janssen PJ, Van Houdt R, Moors H, Monsieurs P, Morin N, Michaux A *et al* (2010). The complete genome sequence of *Cupriavidus metallidurans* strain CH34, a master survivalist in harsh and anthropogenic environments. *PLoS ONE* **5:** e10433.

Kaeberlein T, Lewis K, Epstein SS (2002). Isolating "uncultivable" microorganisms in pure culture in a simulated natural environment. *Science* **296:** 1127-1129.

Kim JY, Kim JK, Lee SO, Kim CK, Lee K (2005). Multicomponent phenol hydroxylase-catalysed formation of hydroxyindoles and dyestuffs from indole and its derivatives. *Lett Appl Microbiol* **41:** 163-168.

Kubista M, Akerman B, Norden B (1987). Characterization of Interaction between DNA and 4',6-Diamidino-2-phenylindole by Optical Spectroscopy. *Biochemistry (Mosc)* **26:** 4545-4553.

Li MQ, Huang WE, Gibson CM, Fowler PW, Jousset A (2013). Stable isotope probing and Raman apectroscopy for monitoring carbon flow in a food chain and revealing metabolic pathway. *Anal Chem* **85:** 1642-1649.

Manefield M, Whiteley AS, Griffiths RI, Bailey MJ (2002). RNA stable isotope probing, a novel means of linking microbial community function to phylogeny. *Appl Environ Microbiol* **68:** 5367-5373.

Marchesi JR, Sato T, Weightman AJ, Martin TA, Fry JC, Hiom SJ *et al* (1998). Design and evaluation of useful bacterium-specific PCR primers that amplify genes coding for bacterial 16S rRNA. *Appl Environ Microbiol* **64:** 795-799.

McDonald D, Price MN, Goodrich J, Nawrocki EP, DeSantis TZ, Probst A *et al* (2012). An improved Greengenes taxonomy with explicit ranks for ecological and evolutionary analyses of bacteria and archaea. *ISME J* **6:** 610-618.

Nelson CE, Carlson CA (2012). Tracking differential incorporation of dissolved organic carbon types among diverse lineages of Sargasso Sea bacterioplankton. *Environ Microbiol* **14:** 1500-1516.

Neufeld JD, Vohra J, Dumont MG, Lueders T, Manefield M, Friedrich MW *et al* (2007). DNA stable-isotope probing. *Nat Protoc* **2:** 860-866.

Pernthaler A, Dekas AE, Brown CT, Goffredi SK, Embaye T, Orphan VJ (2008). Diverse syntrophic partnerships from-deep-sea methane vents revealed by direct cell capture and metagenomics. *Proc Natl Acad Sci U S A* **105:** 7052-7057.

Radajewski S, Ineson P, Parekh NR, Murrell JC (2000). Stable-isotope probing as a tool in microbial ecology. *Nature* **403:** 646-649.

Rappe MS, Giovannoni SJ (2003). The uncultured microbial majority. *Annu Rev Microbiol* **57:** 369-394.

Read DS, Whiteley AS (2011). *Identity and function of single microbial cells within a community by Raman microspectroscopy and related single-cell techniques.*

Rinke C, Schwientek P, Sczyrba A, Ivanova NN, Anderson IJ, Cheng JF *et al* (2013). Insights into the phylogeny and coding potential of microbial dark matter. *Nature* **499:** 431-437.

Schleifer KH (2004). Microbial diversity: Facts, problems and prospects. *Syst Appl Microbiol* **27:** 3-9.

702

703 Schloss PD, Westcott SL, Ryabin T, Hall JR, Hartmann M, Hollister EB *et al* (2009).
704 Introducing mothur: Open-source, platform-independent, community-supported
705 software for describing and comparing microbial communities. *Appl Environ*
706 *Microbiol* **75:** 7537-7541.

707

708 Sun JQ, Xu L, Tang YQ, Chen FM, Wu XL (2012). Simultaneous degradation of
709 phenol and n-hexadecane by *Acinetobacter* strains. *Bioresour Technol* **123:** 664-668.

710

711 Vajrala N, Martens-Habbena W, Sayavedra-Soto LA, Schauer A, Bottomley PJ, Stahl
712 DA *et al* (2013). Hydroxylamine as an intermediate in ammonia oxidation by globally
713 abundant marine archaea. *Proc Natl Acad Sci U S A* **110:** 1006-1011.

714

715 Vartoukian SR, Palmer RM, Wade WG (2010). Strategies for culture of 'unculturable'
716 bacteria. *FEMS Microbiol Lett* **309:** 1-7.

717

718 Wang Y, Chen Y, Zhou Q, Huang S, Ning K, Xu J *et al* (2012). A culture-
719 independent approach to unravel uncultured bacteria and functional genes in a
720 complex microbial community. *PLoS ONE* **7:** e47530.

721

722 Wang Y, Ji YT, Wharfe ES, Meadows RS, March P, Goodacre R *et al* (2013). Raman
723 activated cell ejection for isolation of single cells. *Anal Chem* **85:** 10697-10701.

724

725 Whitman WB, Coleman DC, Wiebe WJ (1998). Prokaryotes: The unseen majority.
726 *Proc Natl Acad Sci U S A* **95:** 6578-6583.

727

728 Zengler K, Toledo G, Rappe M, Elkins J, Mathur EJ, Short JM *et al* (2002).
729 Cultivating the uncultured. *Proc Natl Acad Sci U S A* **99:** 15681-15686.

730

731 Zhang D, Fakhrullin RF, Ozmen M, Wang H, Wang J, Paunov VN *et al* (2011).
732 Functionalization of whole-cell bacterial reporters with magnetic nanoparticles.
733 *Microbial Biotech* **4:** 89-97.

734

735

Figure legends

737 **Figure 1.** Schematic process of recovering live bacteria from their natural
738 environment through magnetic nanoparticle (MNP) functionalisation and separation.

739

740 **Figure 2.** (A) Kinetics of phenol biodegradation in biosludges of good or poor
741 performance (G-BS and P-BS, respectively). Phenol degradation in G-BS was
742 completed in 7 hours (■, ♦ and •) whereas in P-BS phenol degradation completed in
743 36 hours (□, ◊ and o). Neither the use of isotope-labelled phenol (^{13}C-phenol, ♦ and ◊)
744 nor magnetic nanoparticles (MNPs) functionalisation (• and o) had significant impact
745 on bacterial phenol degradation in G-BS and P-BS samples. No phenol degradation
746 occurred without the biosludge (▲ and Δ). A subset of samples were withdrawn from
747 the G-BS incubations with ^{13}C-phenol and ^{12}C-phenol at t= 0, 2.5, 5, 7 hours for
748 DNA-stable isotope probing (DNA-SIP) analyses and the data are presented in
749 Figures 4, S2 and S3.

750 (B) The phenol degradation performances of MRCs (•), the initial biosludges, G-BS
751 (■) and negative controls (▲, no biosludge added).

752

753 **Figure 3.** Raman micro-spectroscopy identification of ^{13}C-stable isotope
754 incorporation into MRCs.

755

756 **Figure 4.** (A) Taxonomy summary of microbial community in the biosludges based
757 on Greengenes 16S rRNA database. SIP experiments indicated that *Burkholderiales*
758 spp. were dominant species in ^{13}C-fraction after 7 h phenol degradation, suggesting
759 they were key phenol degraders *in-situ*.

760 (B) A dendrogram of the bacterial community structures during phenol degradation,
761 using the PCoA (Principle Coordinates Analysis) plot.
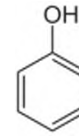
762

763 **Figure 5.** (A) Growth curves of MRCs in the presence of hydroxylamine, ammonia,
764 nitrite or nitrate.

765 (B) The remained phenol concentration after 19 hours during phenol degradation by
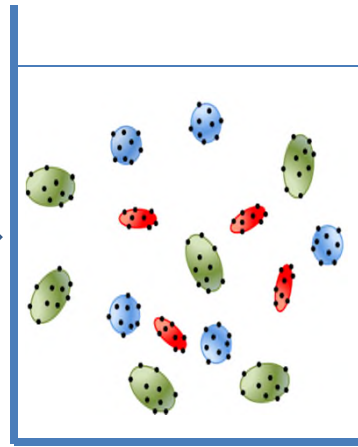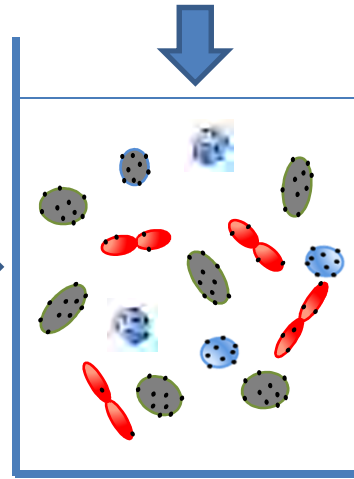766 MRCs.

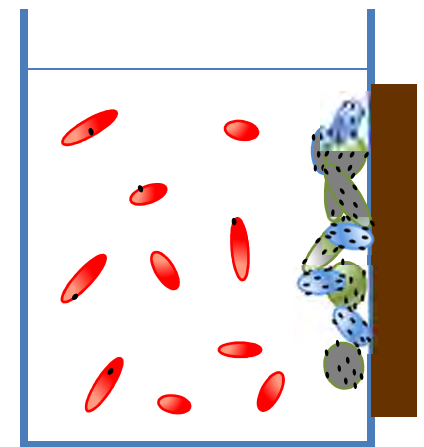767

768

Adding substrate (e.g. carbon source)
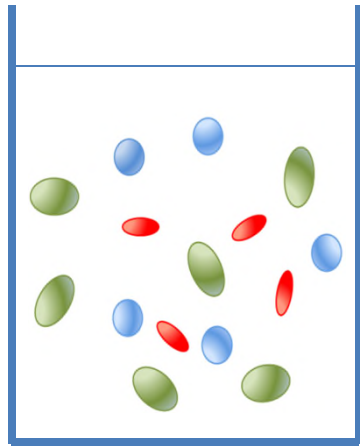
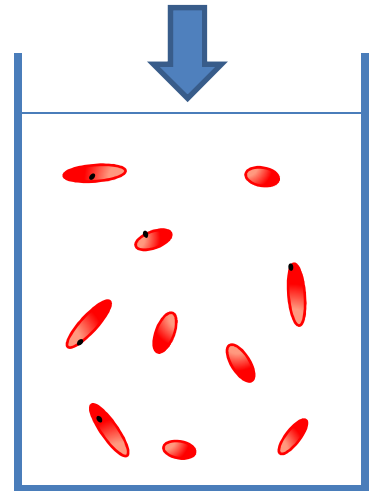1. Original microbial community in a complex system

2. Cells functionalised with MNPs are re-introduced into original condition

3. Active cells dilute MNPs and lose magnetic attraction due to cell dividing

4. Magnetic separation of active and inactive cells

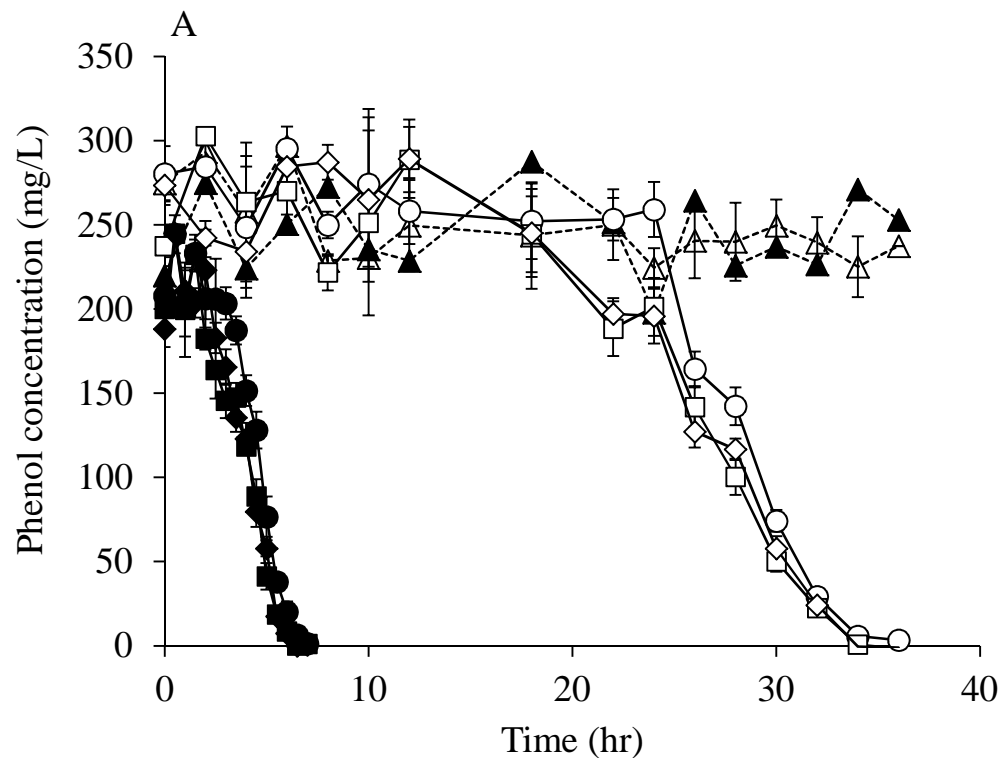5. Collection of live and active cells (e.g. uncultured bacteria)
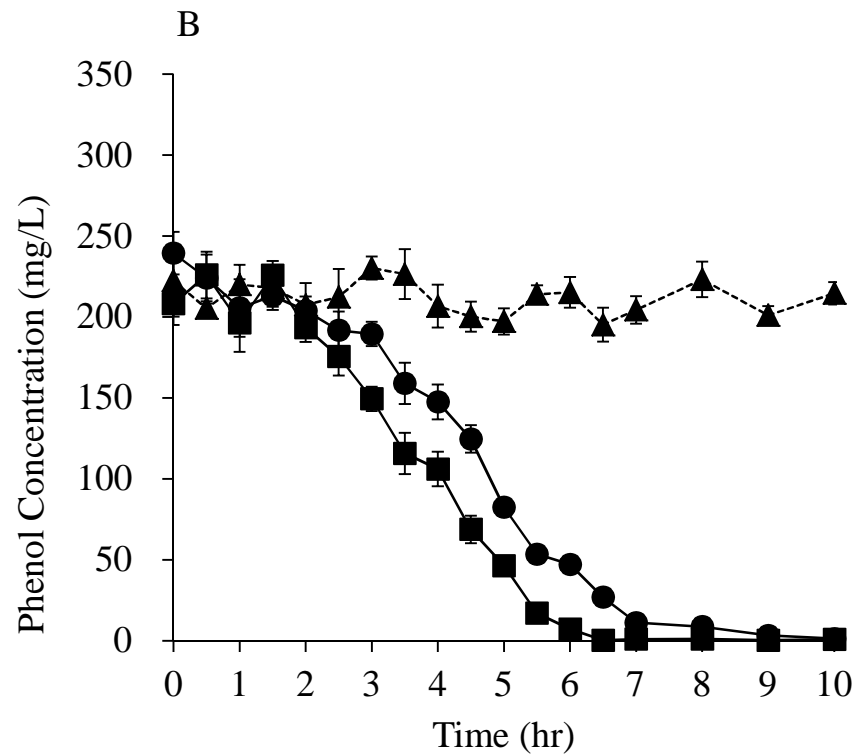
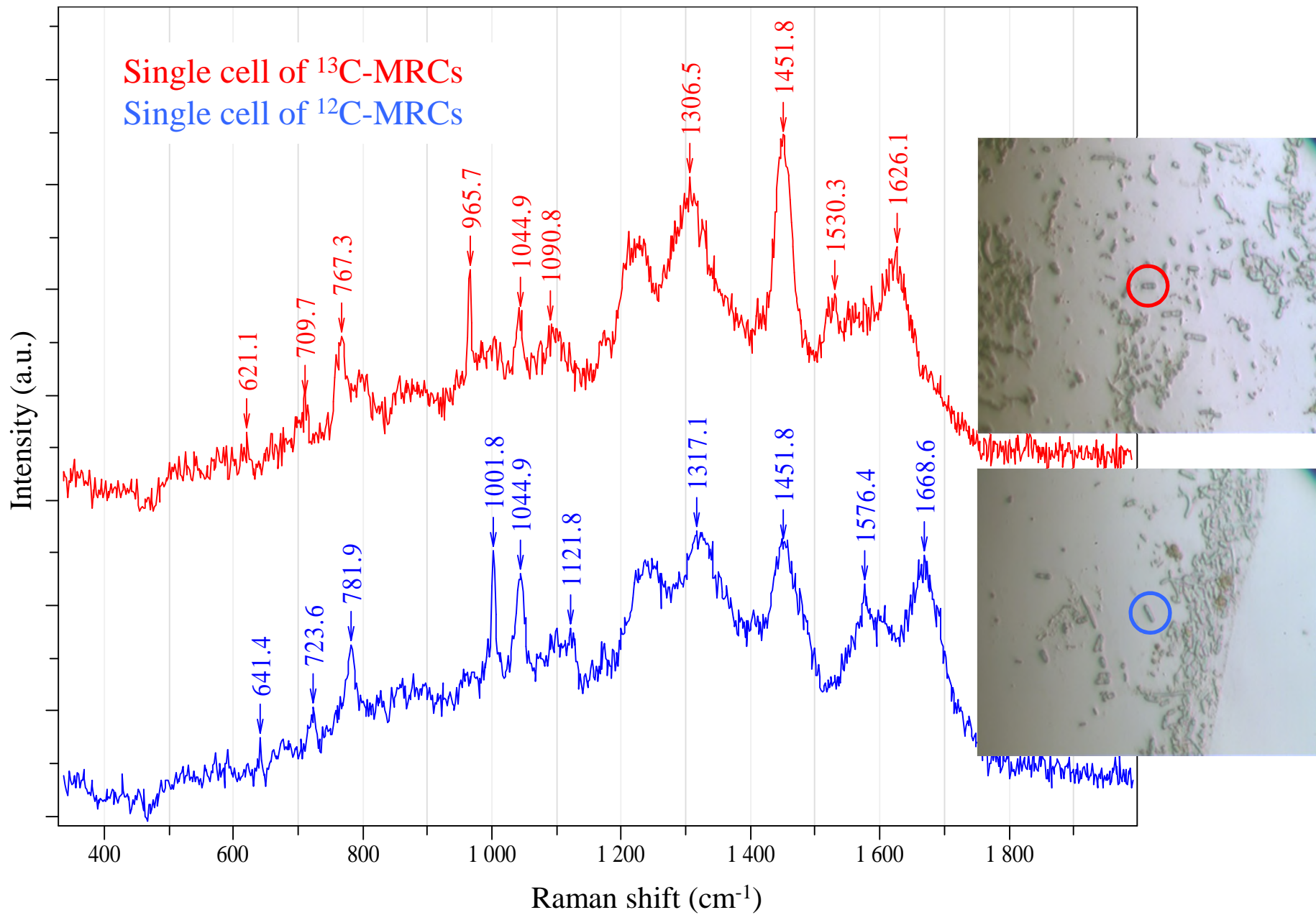Magnetic nanoparticles (MNPs)

Active cells (e.g. uncultured degraders)

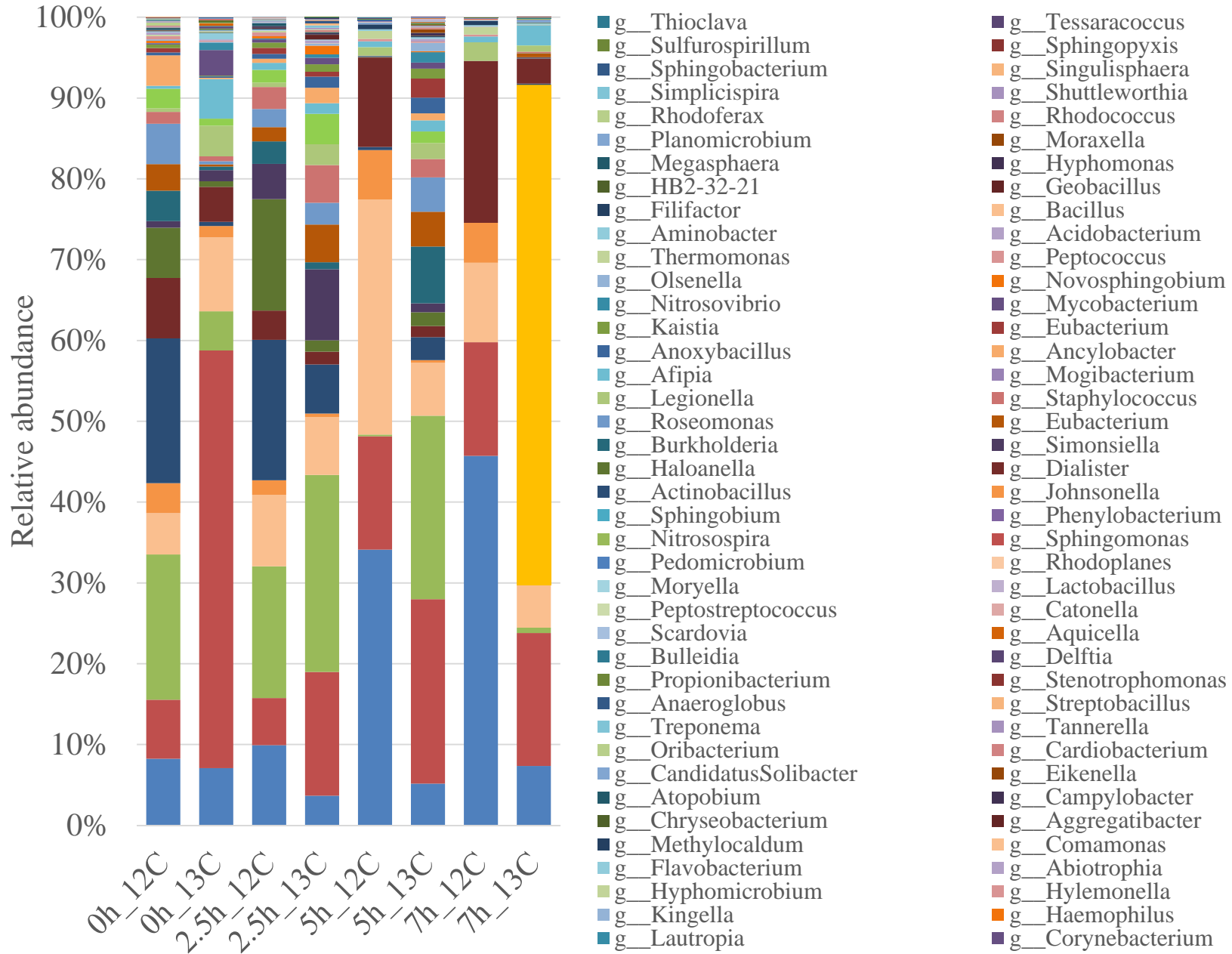Inactive cells (e.g. non-degraders)

Figure legend:

- --▲-- 13C cell-free control
- --△-- 12C cell-free control
- —●— MNPs-G
- —○— MNPs-P
- —■— 12C-G-BS
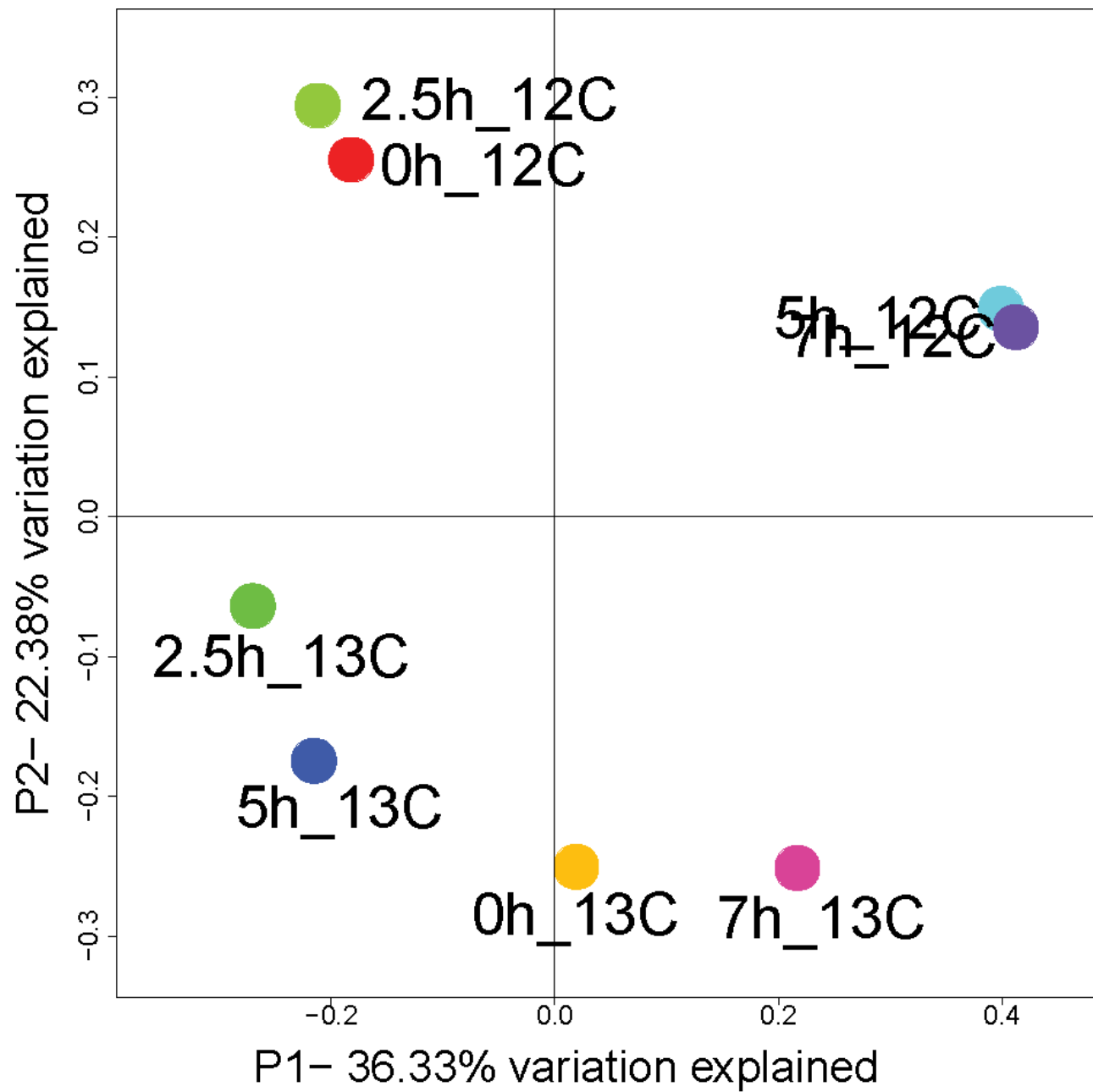- —□— 12C-P-BS
- —◆— 13C-G-BS
- —◇— 13C-P-BS

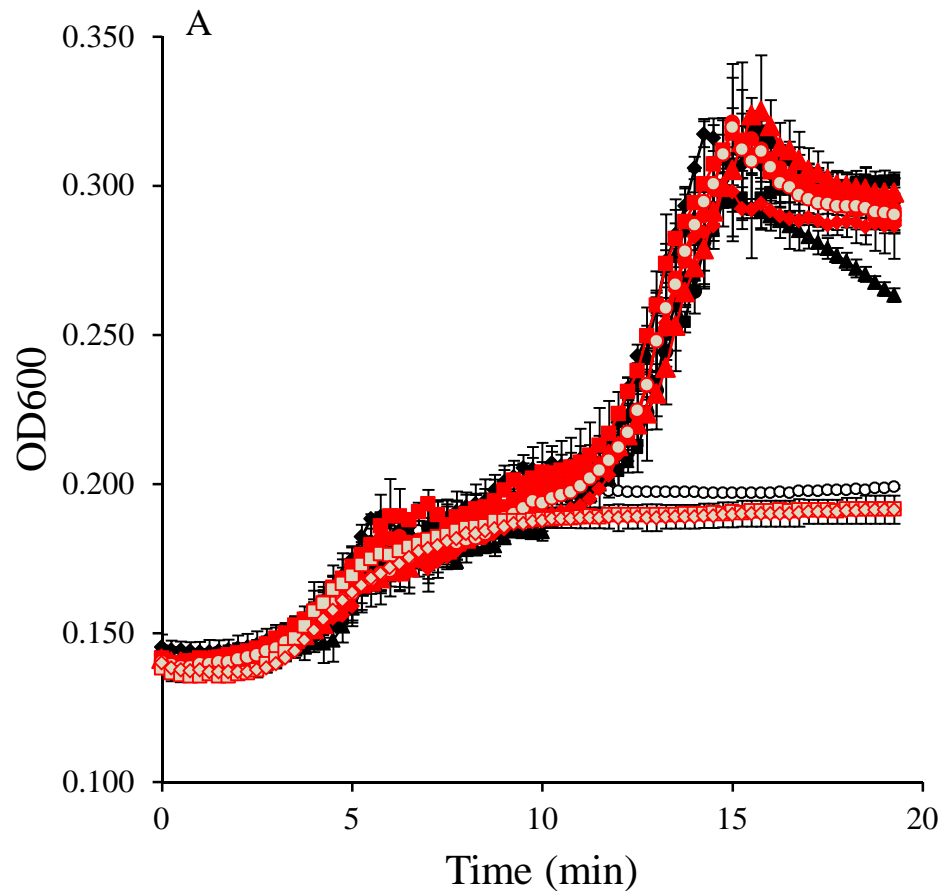- --▲-- Cell-free Control
- —■— G-BS
- —●— MNPs-free cells

A
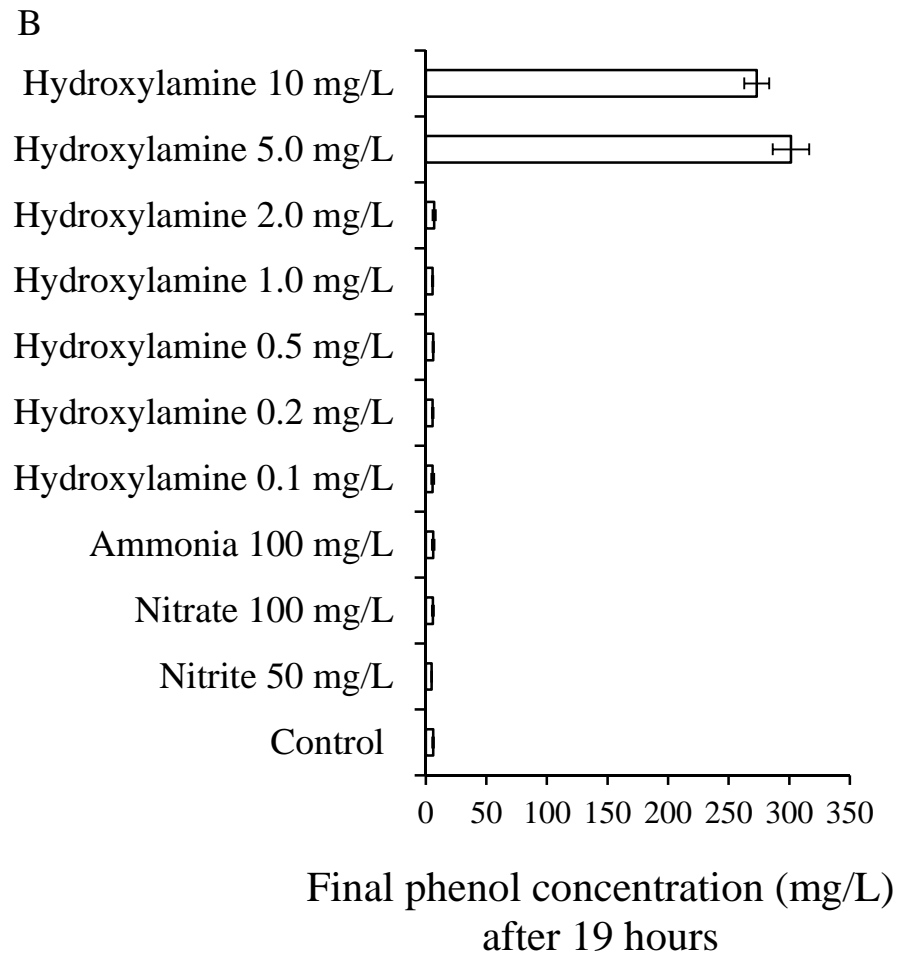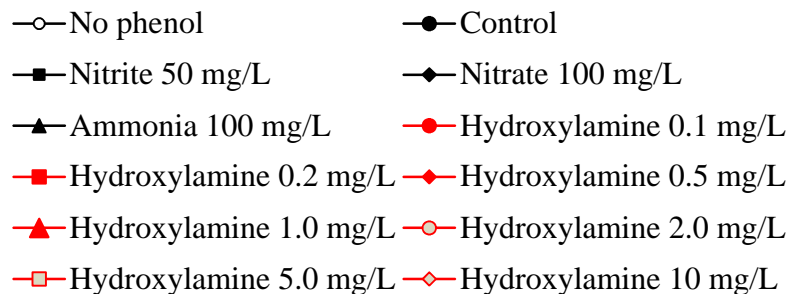
A

B

Hydroxylamine 10 mg/L	
Hydroxylamine 5.0 mg/L	
Hydroxylamine 2.0 mg/L	
Hydroxylamine 1.0 mg/L	
Hydroxylamine 0.5 mg/L	
Hydroxylamine 0.2 mg/L	
Hydroxylamine 0.1 mg/L	
Ammonia 100 mg/L	
Nitrate 100 mg/L	
Nitrite 50 mg/L	
Control	

Final phenol concentration (mg/L)
after 19 hours

—○— No phenol   —●— Control
—■— Nitrite 50 mg/L   —◆— Nitrate 100 mg/L
—▲— Ammonia 100 mg/L   —●— Hydroxylamine 0.1 mg/L
—■— Hydroxylamine 0.2 mg/L —◆— Hydroxylamine 0.5 mg/L
—▲— Hydroxylamine 1.0 mg/L —○— Hydroxylamine 2.0 mg/L
—□— Hydroxylamine 5.0 mg/L —◇— Hydroxylamine 10 mg/L